Suppression of electron acceleration by strong self-amplified magnetic field in quasi-parallel collisionless shocks

Minh Nhat Ly
大阪大学 大学院理学研究科

1. Introduction

Collisionless shocks are ubiquitous phenomena in space and astrophysical plasmas. In the ordinary shockwaves we frequently observe on Earth, energy dissipation is primarily driven by particle collisions. However, the hot and dilute extraterrestrial environments where astrophysical shocks are found are effectively collisionless, as binary particle collisions are rare. Through extensive studies of such systems, most notably Earth's bow shock and supernova remnants, we know that the magnetic field facilitates the dissipation of the shock's kinetic energy via collective interactions with charged particles (see Refs. 1, for a review).

One of the most important properties of collisionless shocks is their remarkable ability to accelerate particles to relativistic energies (2). These "cosmic accelerators" are believed to be responsible for the highly energetic particles, or cosmic rays, detected on Earth (3, 4). Both electrons and ions primarily gain energy through a process known as diffusive shock acceleration (DSA), which involves repeated scattering across the shock front by electromagnetic (EM) waves (2).

The physical characteristics of a shock, and consequently its ability to accelerate particles, are largely determined by the angle, θ_{Bn}, between the shock normal (the direction of shock propagation) and the upstream magnetic field (5). This parameter determines whether the shock is quasi-parallel ($\theta_{Bn} < 45°$) or quasi-perpendicular ($\theta_{Bn} > 45°$). It is well-established that quasi-parallel shocks can efficiently inject both electrons and ions into the DSA cycle, although ion acceleration is significantly more efficient than that of electrons (5, 6). In contrast, while electron acceleration can occur at quasi-perpendicular shocks, the injection of ions into the DSA process has not been observed (5, 7).

Ion acceleration at quasi-parallel shocks is relatively well understood. Ions are reflected from the reforming shock front and stream into the upstream region, forming what is known as the shock precursor. In this precursor, the streaming ions amplify the magnetic field and generate the turbulence necessary to scatter particles back toward the shock (8, 9), which is a crucial step for completing the DSA cycle and preventing their escape.

In contrast, electron acceleration in quasi-parallel shocks is more complex and less understood (10, 11). Due to their much smaller Larmor radii, electrons require significant pre-acceleration before they can be injected into the DSA process. Their acceleration is believed to depend strongly on ion dynamics, as the turbulent fields generated by ions are the dominant mechanism for their energization. Unraveling the mechanisms of electron acceleration is crucial for interpreting astrophysical observations, as electrons are the primary source of the observed non-thermal radiation spectra (12).

In this research, we propose an additional constraint on electron acceleration within the DSA framework. We demonstrate that if the shock drives strong magnetic field amplification, it can become locally superluminal, which in turn suppresses electron DSA. This process is demonstrated self-consistently using first-principles Particle-in-Cell (PIC) simulations.

2. The Particle-in-cell method to study quasi-parallel shocks

In this section, we introduce the Particle-in-Cell

(PIC) method and outlines the simulation setup used to study quasi-parallel collisionless shocks. We will demonstrate two simulation setups: one that results in electron acceleration and one that does not.

2.1. Particle-in-cell method

The Particle-in-Cell (PIC) method is a kinetic approach that models plasma as a large ensemble of discrete macro-particles, representing both ions and electrons (see Ref. 13 for PIC method review). This technique is essential for our research as it facilitates a self-consistent study of the micro-scale physics that fluid-based models, such as magnetohydrodynamics (MHD), cannot resolve (14).

In the PIC method, macro-particles move freely within the simulation domain, driven by the equations of motion. The electromagnetic (EM) field, which provides the Lorentz force, is calculated on a grid. Consequently, macro-particles interact indirectly through the grid-based EM field. This approximation is valid because the plasma is collisionless and binary interactions between particles extremely rare. The feedback of particles for the EM field, charge and current densities, are computed at each time step by summing the contributions of all individual particles onto the grid. This self-consistent loop accurately captures the complex interplay between particle dynamics and wave generation, such as the ion streaming that drives turbulence and the subsequent particle scattering fundamental to the diffusive shock acceleration (DSA) process.

2.2. Simulation setup

The simulations employ the piston method, which models the shock in the downstream rest frame (Fig. 1) (5, 6). We employ public PIC code SMILEI for our calculation (15). Reflective boundary conditions are used for both the macro-particles and the EM fields. The initial plasma is given a drift velocity of $-v_{pt}$ filling the entire simulation domain. This plasma reflects off the boundary on the left. The shock emerges from the interaction between the two counter-streaming flows and propagates to the right. Assuming a strong shock condition (compression ratio r = 4), the shock speed is $v_{sh}{}' = 1/3\, v_{pt}$ in the downstream frame, which corresponds to $v_{sh} = 4/3\, v_{pt}$ in the upstream rest frame.

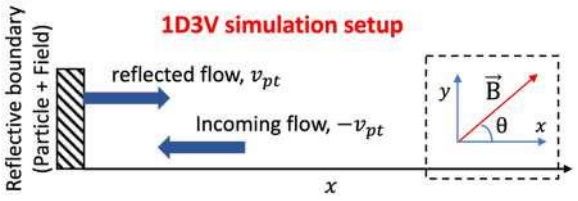

Figure 1. Schematic picture of PIC simulation setup using piston method.

Simulation parameters are summary as follow:

- Domain and Resolution: The simulation domain length is $L_x = 180224\,[c/\omega_{pe}]$, where c is the speed of light and ω_{pe} is intrinsic plasma frequency. The spatial resolution is set to 10 grid cells per electron inertial length c/ω_{pe}. The time step is dt = 0.4 ω_{pe}^{-1} to satisfy the Courant–Friedrichs–Lewy condition (13, 15).

- Physical Parameters: In all simulations, the angle between the magnetic field and the shock normal is fixed at $\theta_{Bn,0}$ = 30°. The magnetic field is initialized as $B_0 = B_0\,[\cos(\theta_{Bn,0})\hat{x} + \sin(\theta_{Bn,0})\hat{y}]$. The injection velocity is v_{pt} = 0.25c, leading to a shock velocity of v_{sh}= 0.33c. The magnetic field strength is set in code units to yield a fixed Alfvén Mach number of $M_A = v_{sh}/v_A$= 26, where v_A is the Alfvén speed.

- Varied Parameter: We vary the sonic Mach number ($M_s = v_{sh}/c_s$,), setting it to M_s = 4 and M_s =20. Here, $c_s = \sqrt{(T_i + T_e)/m_i}$ is the plasma sound speed. We chose to vary M_s because these cases demonstrate different levels of magnetic field amplification. The M_s =20 case, in particular, generates a turbulent field strong enough to suppress electron DSA.

3. Results

3.1. Evidence of electron DSA suppression

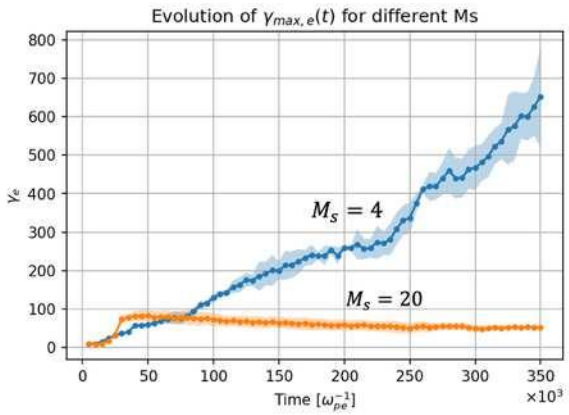

Figure 2. Maximum Lorentz factor $\gamma_{max,e}$ evolving overtime. $\gamma_{max,e}$ was obtained by tracking 10 highest energy electrons in the entire simulation domain and calculating their average γ_e.

In the $M_s = 4$ simulation (blue line in Fig. 2), electrons are continuously accelerated, with their energy steadily increasing throughout the simulation. This linear growth in energy is a classic signature of the Diffusive Shock Acceleration (DSA) mechanism operating effectively.

In simulation with $M_s = 20$ simulation, electrons initially gain energy by pre-acceleration processes, their acceleration halts, and the maximum Lorentz factor plateaus at around $\gamma_e \approx 100$. This stalling of acceleration provides clear evidence that the DSA process has been suppressed for electrons this case. The following sections will explore the physical reason for this suppression.

3.2. Magnetic field amplification

To understand the suppression of electron DSA, we examine the magnetic field structure at the shock. Figure 3 reveals that the $M_s = 20$ shock is associated with significantly stronger magnetic field amplification compared to the $M_s = 4$ case.

Figure 3 a) shows a snapshot of the magnetic field components B_y and B_z for the $M_s = 20$ simulation. The upstream magnetic fluctuation and amplification of perpendicular components ($x - x_{sh} > 0$) is causing by reflected-ions-trigger streaming instability (8). Figure 3 b) quantifies the amplification in the upstream by showing the time-averaged perpendicular magnetic field, $B_\perp = \sqrt{B_y^2 + B_z^2}$. $M_s = 20$ show much stronger amplification than $M_s = 4$ which is consistent with results from previous studies (16). Notably, in the $M_s = 20$ simulation, the amplified magnetic field (orange line) exceeds the theoretical critical threshold required to suppress electron DSA (red dashed line). As will be discussed in the following section, this intense turbulence is the key mechanism that halts the electron acceleration process.

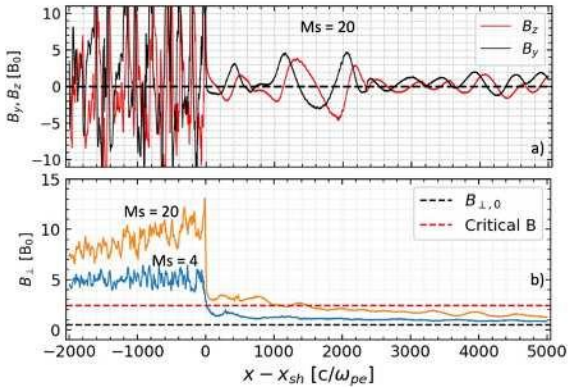

Figure 3. a) Magnetic field profile, B_y and B_z at $t = 225{,}000\ \omega_{pe}^{-1}$ of simulation with $M_s = 20$. b) Time average over $t = 200{,}000 - 250{,}000\ \omega_{pe}^{-1}$ of perpendicular magnetic field, $B_\perp = \sqrt{B_y^2 + B_z^2}$. The magnitude of $B_\perp\ [B_0]$ is compare with initial value $B_{\perp,0}$ and the theoretical critical value from Eq. 1. The position has been normalized with the shock position, x_{sh}.

3.3. Critical field condition

The reason for the suppression of electron DSA in the $M_s = 20$ case is straightforward. For electrons to be injected into the DSA process, they must travel upstream against the plasma flow, scatter off turbulent fields, and return to the shock. Since electrons diffuse primarily along magnetic field lines, their ability to escape upstream is highly dependent on the field's orientation.

If the perpendicular magnetic field is strongly amplified, the angle $\theta_{Bn} = \arccos(B_x/B_{tot})$ will

significantly increase ($B_{tot} = \sqrt{B_{\perp} + B_x}$ is the total field amplitude). The speed an electron must achieve *along the magnetic field line* to outrun the shock front is $v_{sh}/\cos(\theta_{Bn})$. As the electrons velocity cannot exceed the speed of light, if $v_{sh}/\cos(\theta_{Bn}) > c$, the shock will become superluminal and subsequently impossible for electron to escape upstream. Hence, the critical condition for electron DSA is

$$\frac{B_{tot}}{B_0} < \frac{c}{v_{sh}} \cos(\theta_{Bn,0}). \quad (1)$$

4. Discussion and conclusion

In this study, we investigated the impact of the Sonic Mach number (M_s) on the efficiency of electron acceleration in quasi-parallel collisionless shocks. Using 1D Particle-in-Cell (PIC) simulations, we modeled two distinct scenarios: a low Mach number shock ($M_s = 4$) and a high Mach number shock ($M_s = 20$), while keeping other parameters like the Alfvén Mach number constant.

We clearly demonstrate that shock with $M_s = 20$ can drive strong magnetic field amplification, in which case electron DSA is suppressed. This results change common belief that high Mach number shock is always more efficient in particle acceleration (11). In mildly relativistic shocks regime, extreme amplification of magnetic field can significantly dampened electron acceleration process. The suppression is caused by the superluminal shock condition, which was triggered by intense magnetic field amplification in the $M_s = 20$ case. The resulting increase in the field line angle (θ_{Bn}) blocked the electrons' upstream return to the shock, halting the DSA process by violating the critical condition in Eq. (1).

In conclusion, our work has shown by first-principle that electron acceleration might be suppressed by strong self-amplified magnetic field in quasi-parallel collisionless shocks. This finding has important implications for astrophysical environments such as supernova remnants and galaxy clusters, where a wide range of shock Mach numbers is expected. Future work using 2D and 3D simulations would be valuable to confirm if this suppression mechanism persists in higher dimensions.

References

(1) A. Balogh and R. A. Treumann, Physics of Collisionless Shocks: Space Plasma Shock Waves (Springer, NY, 2013).

(2) R. Blandford and D. Eichler, Physics Reports 154, 1 (1987).

(3) L. O. Drury, Astroparticle Physics 39–40, 52 (2012).

(4) P. Blasi, Astron Astrophys Rev 21, 70 (2013).

(5) D. Caprioli and A. Spitkovsky, ApJ 783, 91 (2014).

(6) J. Park, D. Caprioli, and A. Spitkovsky, Phys. Rev. Lett. 114, 085003 (2015).

(7) R. Xu, A. Spitkovsky, and D. Caprioli, ApJL 897, L41 (2020).

(8) A. R. Bell, Monthly Notices of the Royal Astronomical Society 353, 550 (2004).

(9) A. Marcowith, A. J. Van Marle, and I. Plotnikov, Physics of Plasmas 28, 080601 (2021).

(10) S. Gupta, D. Caprioli, and A. Spitkovsky, ApJ 968, 17 (2024).

(11) S. Gupta, D. Caprioli, and A. Spitkovsky, ApJ 976, 10 (2024).

(12) G. B. Rybicki and A. P. Lightman, Radiative Processes in Astrophysics (Wiley-Vch, Weinheim, 2004).

(13) C. K. Birdsall and A. B. Langdon, Plasma Physics via Computer Simulation (McGraw-Hill, New York, 1985).

(14) A. Marcowith, G. Ferrand, M. Grech, Z. Meliani, I. Plotnikov, and R. Walder, Living Rev Comput Astrophys 6, 1 (2020).

(15) J. Derouillat et al., Computer Physics Communications 222, 351 (2018).

(16) D. Caprioli and A. Spitkovsky, ApJ 794, 46 (2014).